Bulletin of the Geological Society of Malaysia, Volume 74, November 2022, pp. 55 - 67
DOI: https://doi.org/10.7186/bgsm74202204

Sulfidation and gold precipitation in the Jugan gold deposit in Bau, Sarawak, East Malaysia: Insights from correlation plots and factor analysis

Aubrey Marie Villareal-Tirona[1,*], Maria Ines Rosana Balangue-Tarriela[1], Ray Shaw[2]

[1] National Institute of Geological Sciences, University of the Philippines, Diliman, Quezon City, Philippines 1101
[2] 45, Besra Gold Inc., Ventnor Ave, West Perth, W.A. Australia 6008
* Corresponding author email address: amvtirona@gmail.com

Abstract: The Jugan Gold Deposit (JGD) is part of the Bau Mineral District (BMD) in Bau, Sarawak, East Malaysia. Although the mineral district is well studied, limited studies were conducted on the JGD. This paper presents the results of statistical studies using the multi-element geochemical data emphasizing the trace elements association with gold, alteration-mineralization, and the precipitation mechanism of the gold-bearing sulfide minerals. The correlation matrix displays positive correlation associations, particularly those associated with gold mineralization, i.e., arsenic, sulfur, antimony, and bismuth. Factor analysis grouped the trace elements into eight factors that reflect lithologies, mineralization, alteration, and geological processes in the JGD. Elements comprising the gold mineralization assemblage have the most significant factor (Factor 1) with the highest variance. The mineral assemblage was enriched during the alteration-mineralization process, as confirmed by the isocon plot. The barren samples (<0.01g/t) and gold-bearing samples (>0.2 g/t) plotted in a Fe vs. S diagram indicate that sulfidation is the precipitation mechanism of gold-bearing sulfide minerals. The immobility of iron and the vertical trajectory trend in the Fe vs. S diagram suggest that the possible source of Fe for gold-bearing sulfide minerals is the sedimentary host rock. Collectively, characteristics such as (1) the association of gold-bearing sulfide minerals with carbonate mineral assemblage and (2) high bismuth loadings on the main mineralization stage suggest a distinct geochemical characteristic of JGD relative to both Carlin-type deposits (CTD) and Carlin-like deposits (CLD); hence it is inferred to be a sedimentary-hosted gold deposit (SHGD). Establishing the JGD characteristics will contribute to a better understanding of the deposit and the BMD. Exploration-wise, it will assist future exploration work in delineating Au mineralization zones.

Keywords: Carlin-type deposits, sedimentary-hosted gold deposits, geochemistry and statistics, gold mineralization, sulfidation, Bau Mineral District

INTRODUCTION

The JGD is situated in BMD, the southwestern corner of Sarawak, East Malaysia. Previous studies by Sillitoe (1986), Majoribanks (1986); Percival *et al*. (1990); Baker (1991); Schuh (1993); Kirwin & Ingram (1993); Garwin (1996) in Mustard (1997) recognized the similarities of BMD to CTD. CTD was first recognized in Nevada in 1961, the Carlin deposit, which initially contained 5 Moz of Au mined through open pit and recovered inexpensively from oxide ore by cyanide leaching (Cline, 2018). In recent years, the genesis and classification of CTDs have remained controversial, and discoveries of similar deposits in different parts of the world led to different terminologies, including Carlin-type, Carlin-like, Carlinesque, sedimentary rock-hosted gold deposits and distal disseminated deposits (Cline, 2018). Hofstra & Cline (2000) were the first to define CTD as a distinct deposit type characterized by four main clusters of deposits (Carlin trend, Getchell, Cortez, and Jeritt Canyon) in Nevada. CTD is defined by (1) carbonate host rocks, (2) tectonic settings associated with passive margins, (3) structural and stratigraphic ore controls, (4) decalcification, silicification, and argillization, (5) Au in solid solution within arsenian pyrite lattices formed by sulfidation, (6) geochemical signature of Au-Tl-As-Hg-Sb-(Te) in ore and ore-stage pyrite with low Ag and base metals, (7) formed at ~180° to 240° C and depths of <~2 to 3 km and (8) absence of a clear relationship with upper crustal intrusion (Hofstra & Cline, 2000). This study will characterize the JGD relative to CTD, CLD, and SHGD.

The JGD was mined in the 1900s by local Chinese to extract eluvial gold. Despite its mining history, studies on the deposit had been limited until Goh's (2012) work on pyrite geochemistry and isotope studies.

The previous works were focused mainly on the large-scale BMD. Schuh (1993), Goh (2012), and Percival *et al*. (2018) reported JGD, as hosted in decalcified, argillized, and weakly silicified carbonaceous shale with submicron Au, contained within the lattices of the sulfides, i.e., arsenian

0126-6187; 2637-109X / Published by the Geological Society of Malaysia.

pyrite and arsenopyrite. Goh (2012) further suggested the association of magmatic-hydrothermal fluids with the deposition of Au. The detailed study by Goh (2012) on pyrite geochemistry suggested two episodes of Au enrichment.

This study utilized statistical methods (correlation matrix, factor analysis, logarithmic isocon diagrams, and bivariate plots) on whole rock geochemistry to determine the trace element and Au association, the migration of elements due to alteration-mineralization, and the precipitation process of Au-bearing sulfides.

METHODS

Description of samples

Samples in this study is from three drill cores that intersect the unmineralized (Figure 1A) and mineralized (Figure 1B) zones of the JGD hosted in various rock types of the Pedawan Formation, which consist of mudrock, sandstone, and intrusive dikes. The sampling technique also involves the collection of samples from the upper and lower zone of the mineralized zone to recognize the transition from the unaltered/ least altered to the altered/ mineralized zone of the deposit.

Statistical analysis

The data used were from the Besra Gold Inc. exploration database. Drill cores were sampled every meter, from 0 m to the end of the hole, and analyzed using ICP for trace elements (Ag, As, Sb, Cu, Pb, Zn, Al, Ba, Bi, Ca, Co, Cr, Fe, Hg, K, Mg, Mn, Na, Ni, Ti, V, and S) and fire assay for Au analyses (n= 892). Half the detection limit was assigned for samples with less than the analytical detection limit.

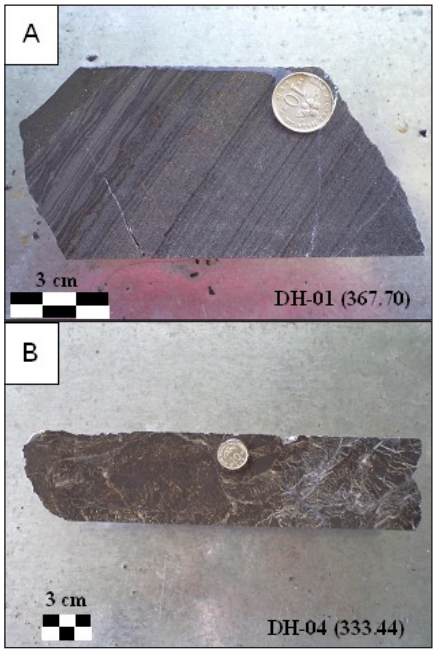

Figure 1: Representative samples of unmineralized (A) and mineralized (B) drill cores from JGD.

Statistical methods employed in this study are factor analysis, correlation matrix, logarithmic isocon diagram, and bivariate plots.

1. Factor analysis (SPSS software) was employed to analyze large geochemical data and group the elements into several factors using principal component analysis as the extraction method, eigenvalue of >1, varimax rotation (orthogonal rotation), and communalities of >0.5. Factor loadings with values >0.5 are considered the major contributing elements in each factor. The different factors will reflect the different geological and geochemical processes in JGD.

2. Correlation matrix (SPSS software) was performed using Pearson correlation at a 95% confidence level to ensure that the true mean of the population value falls within the interval since a large sample size was used. Coefficients considered reliable are <-0.4 and >0.4. This method will display the association of elements with one another.

3. Logarithmic isocon diagram is a method used to correlate movements of trace elements during the alteration process. The initial plan was to perform this method in all rock units; however, no unaltered intrusive sample was encountered. Similarly, sandstone samples are limited. Hence, this method was only employed in mudrock units were the average of five altered and five unaltered mudrock samples were used to determine the gains and losses of the trace elements due to alteration-mineralization in the host rock; and

4. Bivariate plots of Fe *vs.* S diagram for barren samples (<0.01 g/t Au), and Au-bearing samples (>0.2g/t Au) with respect to the pyrite line, S = 1.15 * Fe (wt%) from Stenger *et al.* (1998), will determine the precipitation mechanism of Au-bearing sulfide minerals in Jugan.

REGIONAL GEOLOGY

Borneo lies at the center of the Southeast Asian region, surrounded by Cenozoic subduction zones as a result of the Indian-Australian, Pacific, and Philippine Sea plates convergence (Hall *et al*., 2008). It is bounded by three marginal continental basins: Celebes, Sulu, and the South China Sea, and by the Philippine and Indonesian archipelagos. The general geologic map of Borneo is shown in Figure 2.

North and east Borneo have an ophiolitic basement with possibly older crust intruded by diorite and granites. Thick Cretaceous sedimentary sequences predominantly cover the basement of Borneo. Central Borneo Mountains and Crocker Ranges are formed by the Rajang Group of the Upper Cretaceous-Eocene age consisting of deep marine sediments overlain by Eocene to Lower Miocene turbidites and mudstones (Hutchison, 1996; Van Hattum, 2005). During the Early Miocene, there was a cessation in the deposition of deep-marine sedimentation concurrent with the collision of micro-continental fragments with the western edge of Borneo. This event was followed by the deposition of

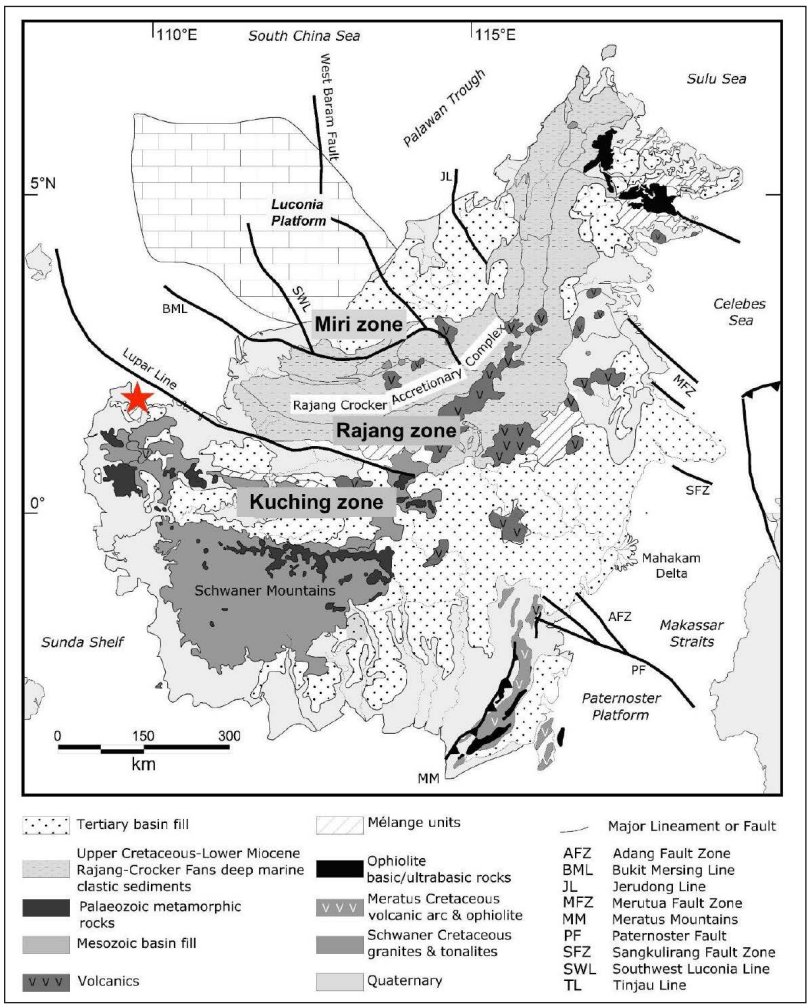

Figure 2: Geologic map of Borneo Island from Hall *et al*. (2008) showing the different rock types and significant lineaments. The red star is the location of the JGD.

siliciclastic sediments along the marginal basins (Hamilton, 1979; Hall & Nichols, 2002). In southwest Borneo (west of Kalimantan), Cretaceous granites and volcanic rocks (Hutchison, 2005) intrude the metamorphic rocks of the Schwaner Mountains.

Numerous sedimentary basins were formed in different geologic settings surrounding the Island (Hall *et al*., 2008). Beneath North Borneo, there is southward subduction of the Proto South China Sea while rifting occurred in the East, forming the Makassar Strait. Simultaneously, complex rifting and extension continued happening in the north and northwest of the island. Afterwards, arc-continent collision in the North resulted in the collision and uplifting in the Central part and inversion of sedimentary basins in Makassar Straits and along the margins of Celebes, Sulu, and the South China Sea.

LOCAL GEOLOGY

JGD is part of the BMD, which hosts several different mineralization styles. It is bounded by the east-northeast Tubah fault in the north and Traan Staat fault in the south. Several northwest-trending faults intersect the BMD. A general geologic map showing the lithologies, structures, and location of the different mineral deposits in BMD is presented in Figure 3, while Figures 4 and 5 illustrate the geologic map of JGD and the simplified stratigraphic column of BMD as described by Wolfenden (1965) and Schuh (1993), respectively.

Serian Volcanics, the oldest rock unit in the district, comprises Upper Triassic age basaltic lava with layers of tuffs, andesite flows, amygdaloidal lavas, and pyroclastic breccias. Unconformably overlying the Serian Volcanics is the Upper Jurassic to Upper Cretaceous Bau Limestone Formation, consisting of the Krian Member and the Bau Limestone Member. The Krian Member, the lower member of the Bau Limestone Formation, consists mainly of impure, light to medium gray-brown sandstone, minor pebbly strata, shale, and argillaceous limestone. In contrast, the Bau Limestone Member is massive with beige to white pure micritic limestone with skeletal foraminifera and algae bioclasts. Conformably overlying the Bau Formation is

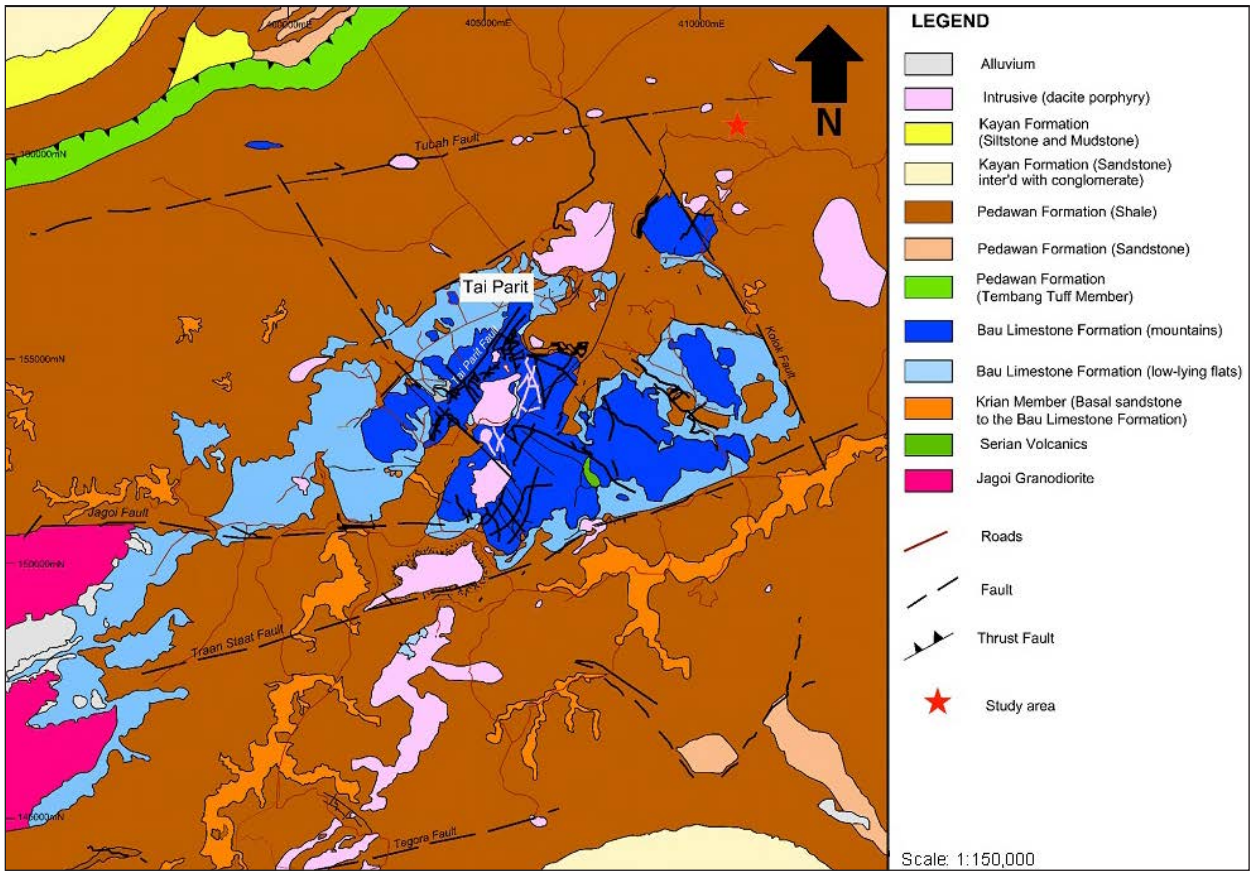

Figure 3: General geologic map of the Bau mineral district. Modified from Banks, 2006.

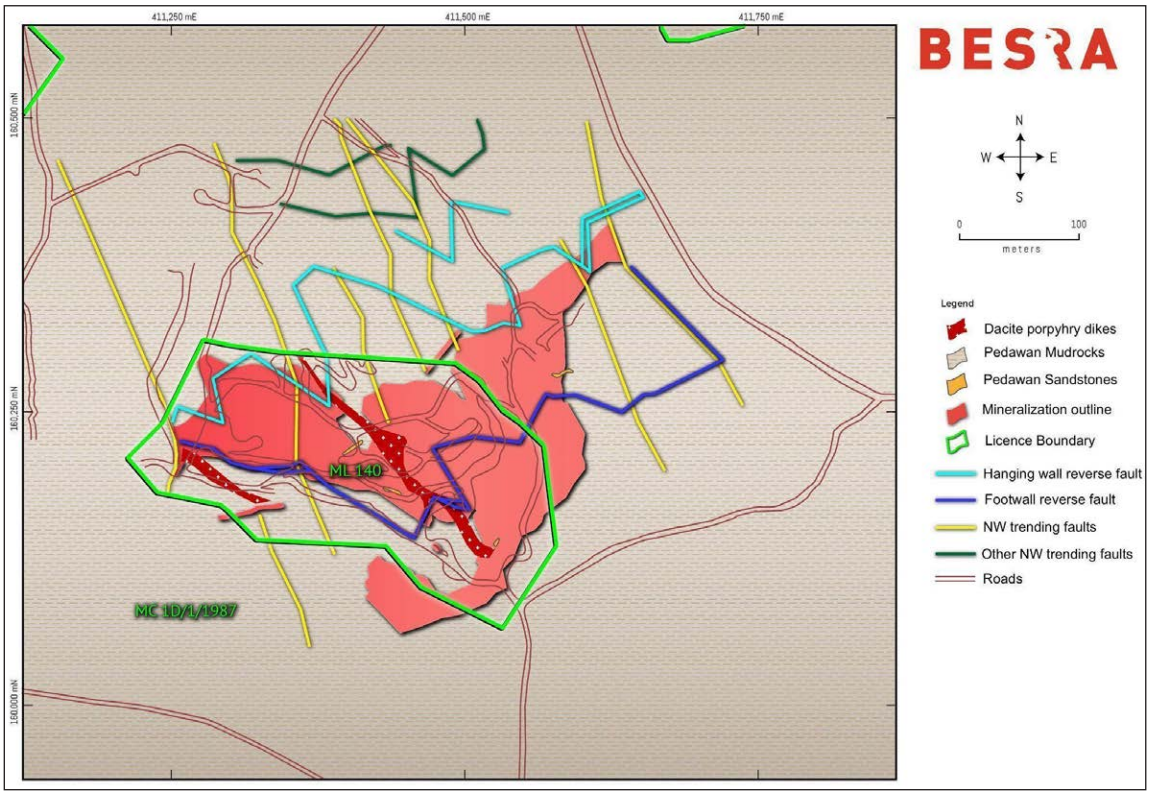

Figure 4: Geologic map of the Jugan gold deposit (Besra Gold Inc., 2022).

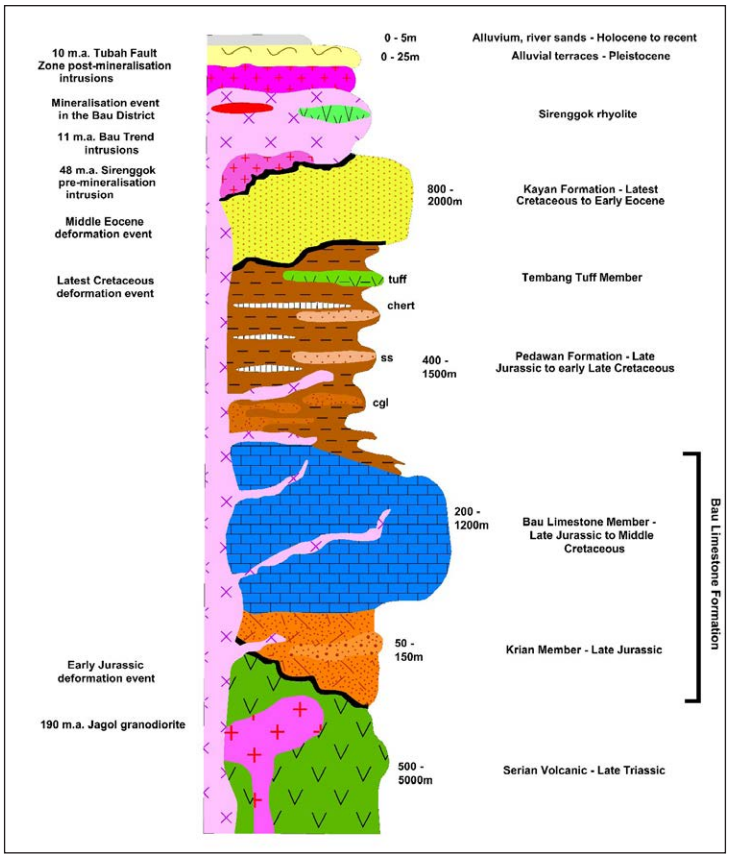

Figure 5: Generalized stratigraphy of the Bau District. Modified from Pour *et al*. (2013). Not to scale.

the thick layer of tightly folded clastic marine sedimentary rocks of the Lower Cretaceous Pedawan Formation dissected by intensely altered intrusive dikes. Serian Volcanics, Bau Limestone, and Pedawan Formations are commonly intersected by acidic to intermediate dikes, with the sole exception of stock in the Taiton area that is classified as dolerite. All intrusive rocks in the district are Mid-Miocene age (JICA, 1985; Goh, 2012) in age and typically irregularly shaped stocks oriented sub-vertical to vertical with parallel northwest and north orientations.

RESULTS

With the permission of Besra Gold Inc., whole-rock geochemistry and fire assay data for 22 elements and fire assay analysis for Au of the 892 samples from three drill holes were used in this study to determine the geochemical signatures of the JGD.

Factor analysis

Factor analysis was employed to compress a large number of data into fewer factors based on linear correlation. The elemental contribution to each factor is quantified by the loading values that display geologic and geochemical associations. Factor analysis generated eight factors that account for 71.84% of the data set, as shown in Table 1. Also, the major contributing elements with factor loadings greater than 0.5 are shown in Table 2, listed in decreasing factor loadings and the total percentage variance for each factor.

Each factor reflects lithologies, mineralization, alteration types, and processes in the JGD.

- Factor 1 (*Au mineralization factor*) has the highest variance consisting of high loadings of Au, As, Sb, Bi, and S.
- Factor 2 (*base metal factor)* comprises high loadings of Cu, Co, and Ni.
- Factor 3 (*intrusive factor*) has high loadings of Ti and Al. Generally; all intrusive units in Jugan have the highest values of Ti (100 ppm - 4,130 ppm). The highest values of Al (7,780 ppm - 17,300 ppm) are also in the intrusive unit.
- Factor 4 (*sedimentary host rock factor*) with high V, Fe, and Na loadings represents the sedimentary host rock factor.
- Factor 5 (*carbonate factor*) has high loadings of Ca, Mg, and Mn elements.
- Factor 6 (*post-mineralization depositional factor*) has high loadings of Ba, and K.
- Factor 7 (*Pb factor*) has the highest loading of Pb.
- Factor 8 (*supergene factor*) has a high loading of Ag, and the highest Ag values are encountered at shallow depths.

Table 1: Association of elements in an eight-factor model in the Jugan gold deposit.

Elements	Factor 1	Factor 2	Factor 3	Factor 4	Factor 5	Factor 6	Factor 7	Factor 8	Communalities
Au	0.838	-0.148	-0.045	-0.172	0.002	0.073	-0.034	0.002	0.763
Ag	0.126	-0.021	0.005	-0.011	0.059	0.065	0.258	0.792	0.717
As	0.946	0.054	-0.080	-0.191	-0.010	-0.065	0.009	-0.024	0.945
Sb	0.737	0.305	-0.116	-0.022	0.099	-0.200	0.038	0.029	0.703
Cu	0.167	0.536	0.498	0.277	0.088	-0.022	0.134	0.050	0.668
Pb	-0.043	0.016	0.005	-0.031	-0.054	-0.024	0.873	0.058	0.772
Zn	0.050	0.439	-0.452	0.312	-0.119	0.304	-0.032	0.039	0.605
Al	-0.241	-0.186	0.521	0.395	-0.272	0.426	0.062	-0.048	0.782
Ba	-0.235	0.048	-0.061	0.084	0.091	0.717	0.070	-0.059	0.599
Bi	0.910	-0.008	0.177	-0.086	-0.039	0.055	-0.020	-0.013	0.872
Ca	-0.109	-0.277	0.004	-0.152	0.778	-0.040	-0.094	-0.002	0.727
Co	0.051	0.845	-0.030	0.034	-0.009	0.111	0.003	-0.011	0.731
Cr	-0.064	0.025	0.712	-0.108	-0.048	-0.006	-0.059	-0.023	0.529
Fe	-0.006	0.267	-0.096	0.730	-0.169	-0.103	0.121	-0.080	0.673
Hg	0.202	-0.045	-0.012	-0.021	0.101	0.127	0.349	-0.590	0.539
K	0.094	0.298	0.283	0.066	0.050	0.728	-0.115	0.047	0.731
Mg	0.126	0.294	-0.044	0.206	0.760	0.135	0.063	0.013	0.747
Mn	-0.022	0.402	-0.042	-0.345	0.692	0.055	-0.018	-0.046	0.767
Na	-0.178	-0.148	0.033	0.592	-0.024	0.243	-0.184	0.109	0.511
Ni	0.111	0.891	0.150	-0.175	0.217	0.097	-0.020	0.008	0.916
Ti	0.108	0.135	0.816	0.242	-0.004	0.179	0.032	0.061	0.792
V	-0.317	-0.099	0.241	0.709	0.041	0.121	-0.026	-0.016	0.688
S	0.705	0.366	0.065	0.082	-0.038	-0.315	0.042	-0.017	0.745

Extraction method: principal component analysis, rotation method: varimax with Kaiser normalization.

Table 2: Major contributing elements in each factor in decreasing factor loadings. Factor loading values considered are >0.5.

Factor 1	Factor 2	Factor 3	Factor 4	Factor 5	Factor 6	Factor 7	Factor 8
Au	Ni	Ti	V	Mg	K	Pb	Ag
As	Co	Cr	Fe	Ca	Ba		
Bi	Cu	Al	Na	Mn			
Sb							
S							
% Total variance of each factor							
19.95	*14.23*	*10.46*	*7.86*	*5.67*	*4.81*	*4.48*	*4.39*

Correlation matrix

Correlation matrix in Table 3 shows the positive correlation between elements such as As-Bi (0.877), Au-As (0.799), Au-Bi (0.785), Co-Ni (0.764), Sb-S (0.719), As-Sb (0.711), As-S (0.684), Cu-Ti (0.561), Bi-S (0.554), Sb-Bi (0.544), Cu-Ni (0.543), Mn-Ni (0.538), Al-Ti (0.520), Al-V (0.508), Au-Sb (0.471), Cr-Ti (0.414), Na-V (0.413) and Ca-Mn (0.402). A negative correlation was noted on As-V (-0.444) and Sb-Al (-0.427). Elements associated with Au mineralization (Factor 1) illustrate a strong positive correlation with each other. Similarly, elements associated with the base metal factor (Factor 2), sedimentary host rock (Factor 4), and carbonate alteration (Factor 5) display a strong positive correlation with one another.

Logarithmic isocon diagram

Logarithmic isocon diagram plots for the host rock (Figure 6) strongly suggest the interpretation that elements with the highest variance (Factor 1 - Au, As, Sb, Bi and S) were all added to the system during alteration-mineralization. Similarly, elements (Ca, Mg and Mn) in Factor 5 are enriched, a relationship that coincides with the carbonate studies of Goh (2012), inferring that carbonate minerals were introduced in the system by the hydrothermal fluids. Base metals, Pb, Co, and Zn, are immobile, while Cu and Ni show subtle enrichment. Fe, a significant element in the formation of sulfide minerals, is immobile in Jugan. Most of the depleted elements (Al, Na, V, Cr, and T) belong to Factors 3 (intrusive) and 4 (sedimentary).

Bivariate plot (Fe vs. S)

The sulfide minerals in Jugan illustrate different morphologies (framboidal, cubic, and subhedral forms) and characteristics (dissemination in the host rock, isolated crystals, association with carbonaceous matter, association with carbonate minerals) that are strong evidence suggesting various episodes of sulfide formation. Also, the varying correlations between sulfide minerals and Au values strongly indicate multiple sulfide mineralizations in Jugan, and not all are associated with Au. To further elucidate the sulfide mineralization, a Fe *vs.* S correlation diagram modified from Stenger *et al*., 1998 and Li *et al*., 2019 was constructed and is shown in Figure 7.

The barren (<0.01 g/t) and Au-bearing samples (>0.2 g/t) were plotted in a correlation diagram to determine the processes involved in the precipitation of sulfide minerals and their possible association with Au. The barren samples plotted between Fe values of 3% to 5% and S values of <2%, while the Au-bearing samples show a strong positive correlation between Fe (3% to 5%) and S (1.5% to 5%) values with $R^2 = 0.4$.

There are two discernable groupings: (1) Group 1 consists of samples found to cluster at low S but a wide range of Fe values, and (2) Group 2 is made up of samples with a similar range of Fe values as Group 1 but an evident parallel displacement to the S axis.

DISCUSSION

Geochemical signatures

The main Au mineralizing event in Jugan comprise Au, As, Sb, Bi, and S assemblage (Factor 1). Isocon plots similarly suggest that these minerals are enriched during alteration-mineralization. The elemental suite of the primary Au mineralization in JGD displays similarities with the geochemical signatures of Au mineralization of CTD, except for the high Bi loading. Bi in CTD is acknowledged but is not directly associated or weakly correlated with Au mineralization. At Jerritt Canyon, Nevada, Bi postdates the deposition of Au-bearing arsenian pyrite and marcasite (Patterson *et al*., 2011). However, and by contrast, Bi, Ag, Pb, Sb, Cu, and Sn are enriched in some pyrite samples associated with high Au values in Jugan (Goh, 2012).

Factor 2 (Ni, Co, and Cu) is the base metal suite that is immobile and subtly enriched in the system. It is possibly sourced from the carbonaceous mudrocks, with an appreciable amount of organic matter (Sethi & Schieber, 1998) because the host rock is a marine sediment deposit. Likewise, diagenetic pyrite is enriched with these base metals (Goh, 2012), which may have contributed to this factor. CTD have low base metals, particularly in the ore and ore stage pyrite (Hofstra & Cline, 2000; Cline, 2018).

The intrusive factor (Factor 3) consists of Ti, Cr, and Al. Ti values in the intrusive rocks are elevated compared with the sedimentary host rock.

Factor 4 (host rock factor) consists of V, Fe, and Na. Vanadium is a common element in carbonaceous shale, particularly during deposition and diagenesis (Breit & Wanty, 1991). Similarly, Fe is abundant in mudrocks because of the carbonaceous material and diagenetic pyrite. Na is also enriched in sedimentary units, particularly those formed in marine environments. Hence, the depletion of V and Na, as shown from the isocon diagram, suggests that it may have been affected by the alteration-mineralization processes. On the other hand, Fe remains immobile during the alteration-mineralization processes.

Factor 5 (carbonate alteration factor) consists of Ca, Mg, and Mn. Several alteration processes were recognized by Villareal-Tirona (2022) in JGD, i.e., silica-clay, carbonate, and argillic alterations where carbonate alteration strongly associates with Au-bearing sulfide minerals. Carbonate minerals in Jugan are generally ankerite in composition with minor calcite and ferroan dolomite (Goh, 2012) occurring as veins and replacement (Figure 8A & B). Petrographic studies by Villareal-Tirona (2022) suggest that carbonate minerals are syngenetic with the Au-bearing sulfide minerals, particularly pyrite (Figure 8C) and arsenian pyrite (Figure 8D). Goh (2012) suggests that carbonate in JGD is hydrothermal in origin. Isocon plots show that Ca, Mg and Mn were enriched during the alteration-mineralization

Table 3: Correlation matrix of 24 elements at a confidence level of 95%. Coefficients considered reliable are ≤-0.4 and ≥ 0.4.

	Au	**Ag**	**As**	**Sb**	**Cu**	**Pb**	**Zn**	**Al**	**Ba**	**Bi**	**Ca**	**Co**	**Cr**	**Fe**	**Hg**	**K**	**Mg**	**Mn**	**Na**	**Ni**	**Ti**	**V**	**S**
Au	1.000																						
Ag	0.055	1.000																					
As	**0.799**	0.083	1.000																				
Sb	**0.471**	0.108	**0.711**	1.000																			
Cu	-0.006	0.053	0.057	0.260	1.000																		
Pb	-0.004	0.034	-0.003	-0.008	0.082	1.000																	
Zn	-0.029	0.009	0.035	0.093	0.115	-0.001	1.000																
Al	-0.241	-0.023	-0.357	**-0.427**	0.186	0.020	-0.054	1.000															
Ba	-0.203	-0.019	-0.277	-0.158	-0.011	-0.002	0.131	0.295	1.000														
Bi	**0.785**	0.051	**0.877**	**0.544**	0.192	-0.003	-0.026	-0.133	-0.212	1.000													
Ca	-0.029	-0.003	-0.076	-0.137	-0.177	-0.061	-0.179	-0.199	0.025	-0.085	1.000												
Co	0.001	0.032	0.104	0.227	0.335	0.026	0.338	-0.115	0.106	0.080	-0.169	1.000											
Cr	-0.047	0.014	-0.069	-0.057	0.130	-0.015	-0.200	0.256	0.030	0.062	0.022	0.030	1.000										
Fe	-0.150	-0.020	-0.085	-0.018	0.140	0.054	0.282	0.241	0.092	-0.053	-0.281	0.259	-0.037	1.000									
Hg	0.097	-0.007	0.163	0.124	0.050	0.001	0.000	-0.007	0.008	0.110	0.013	0.030	-0.018	-0.035	1.000								
K	0.004	0.020	0.017	-0.005	0.268	-0.053	0.207	0.357	0.335	0.130	-0.056	0.266	0.167	0.028	0.006	1.000							
Mg	0.031	0.031	0.078	0.229	0.242	0.006	0.161	-0.178	0.139	0.062	0.298	0.213	-0.071	0.108	0.042	0.256	1.000						
Mn	0.033	0.003	0.078	0.154	0.128	-0.039	0.001	-0.301	0.108	-0.012	**0.402**	0.305	-0.027	-0.210	0.051	0.106	0.507	1.000					
Na	-0.212	-0.009	-0.331	-0.232	0.122	-0.073	0.109	0.330	0.178	-0.205	-0.044	-0.020	-0.055	0.154	-0.054	0.178	-0.038	-0.241	1.000				
Ni	0.028	0.031	0.167	0.295	**0.543**	-0.010	0.253	-0.208	0.039	0.151	-0.041	**0.764**	0.088	0.037	0.037	0.391	0.380	**0.538**	-0.185	1.000			
Ti	-0.017	0.057	-0.029	-0.071	**0.561**	0.005	-0.105	**0.520**	0.073	0.243	-0.101	0.101	**0.414**	0.097	-0.004	0.370	0.125	-0.081	0.155	0.215	1.000		
V	-0.291	-0.037	**-0.444**	-0.274	0.148	-0.015	0.094	**0.508**	0.198	-0.282	-0.025	0.010	0.200	0.390	-0.071	0.138	0.055	-0.225	**0.413**	-0.166	0.247	1.000	
S	0.384	0.075	**0.684**	**0.719**	0.319	0.009	0.056	-0.255	-0.260	**0.554**	-0.141	0.273	0.009	0.217	0.111	0.011	0.071	0.074	-0.174	0.331	0.135	-0.305	1.000

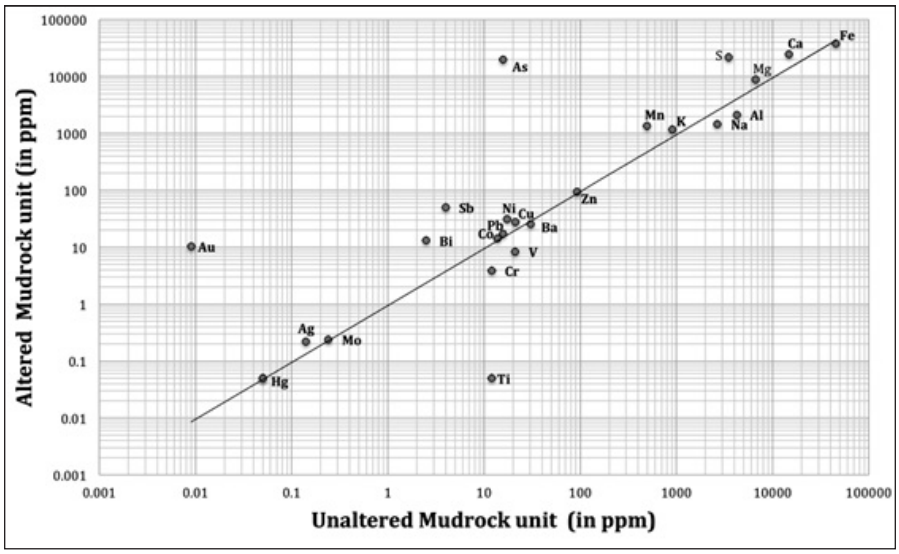

Figure 6: Logarithmic isocon diagram plot showing the movement of elements during the alteration-mineralization process.

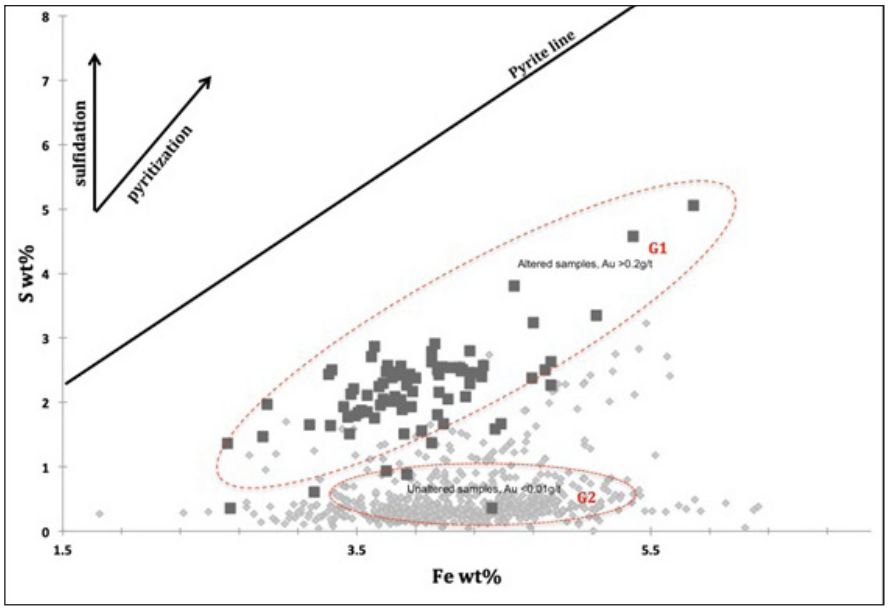

Figure 7: Correlation diagram showing the Fe (wt%) and S (wt %) relationship (modified from Li, 2019). The pyrite line is based on the relative contents of sulfur and iron in pyrite: S = 1.15 * Fe (wt%) from Stenger *et al*., 1998.

process. The negative Fe loading in Factor 5 suggests that Fe is not associated with the elements of the carbonate alteration factor, which is unlikely since Fe is a significant element related to ankerite and ferroan dolomite. Results of factor analysis grouped Fe with other elements representing the sedimentary host rock, while the isocon plot suggests that Fe is immobile during the alteration-mineralization process. It is inferred that the immobile Fe may have reacted with the elements of the carbonate alteration factor during alteration-mineralization forming the carbonate minerals.

Factor 6, or the post-mineralization factor, consists of Ba and K. Ba is associated with the post-ore depositional process in Cortez Hill district, Nevada (Venendaal, 2007). Ba in several CTD in Nevada and CLD in China, in the form of barite, are gangue minerals occurring together with quartz and calcite (Li & Peters, 1998).

Factor 7 (Pb factor) is enriched in the diagenetic pyrite and the early-stage arsenopyrite (Goh, 2012) and does not show any association with Au mineralization. The isocon diagram suggests that Pb in Jugan is immobile.

Factor 8 (Ag factor) is inferred as a supergene event. The weak correlation of Au-Ag observed at Jugan is similar to CTD in Nevada, wherein Ag is low in the ore and ore-stage pyrite (Cline, 2018). The high values of Ag (1.1ppm-1.7ppm) encountered from the drill holes are restricted at shallow depths (0-50m), where samples are generally intensely weathered and oxidized.

Formation of sulfide minerals

All samples plotted below the pyrite line in the Fe *vs*. S graph indicate that sedimentary rock lacks Fe to combine with all the sulfur to form pyrite (Stenger *et al*., 1998). Furthermore, Fe needed to form sulfides may have been sourced from the host rock (Li *et al*., 2019), which conforms to the results of isocon plots suggesting that Fe is immobile. Also, Fe is grouped with elements belonging to the host rock factor (Factor 4).

In the Fe *vs*. S graph, Group 1 shows the bulk of the unmineralized samples suggesting pre-Au mineralization event association. The vertical displacement of Group 2 shows the compositional change associated with sulfidation. Most of the Au-bearing samples fall well within Group 2, suggesting that sulfidation is the principal precipitation mechanism of the Au-bearing sulfide minerals. During sulfidation, the Fe in the host rock is sulfidized by the S-rich hydrothermal fluid together with other metallogenic elements to form sulfide minerals (Li *et al*., 2019). Another scenario could be existing pre-ore pyrite as the core for the sulfidation processes, subsequently forming rims high in As and Au (Hofstra & Cline, 2000). In CTD, the carbonate dissolution process liberates Fe, hence becoming available to react with the ore fluids to form Au-bearing sulfide minerals (Stenger *et al*., 1998). A possible reaction during sulfidation is a co-precipitation with arsenian pyrite, as presented in equation 1 (Simon *et al*., 1999 in Hofstra & Cline, 2000).

Equation 1

$0.3H_3As_3S_6 + 2Au(HS)^0 + Fe^{+2} + 1.5H_2 = Fe(S,As)_2\text{-}Au_2S + 2H_2S + 2H^+$

In Jugan, since carbonate dissolution is absent, the possible sources of Fe needed for the precipitation of sulfide minerals are the carbonaceous matters liberated by the circulating hydrothermal fluid.

CTD, CLD and SHGD vs. JGD

Geochemical and statistical studies in JGD suggest that trace elements associated with Au are As, S, Sb, and Bi. CTD is characterized by Au-Tl-As-Hg-Sb-(Te) geochemical signature (Hofstra & Cline, 2000). Hg in JGD is not associated with Au, while elements Tl and Te were not part of the ICP analysis of Jugan samples. Carbonate alteration, as represented by Ca, Mg, and Mn elements, is inferred to be associated with Au-bearing sulfide minerals in JGD. Although statistical analysis shows a weak correlation between elements of carbonate assemblage and Au, petrographic studies suggest that Au-bearing sulfide

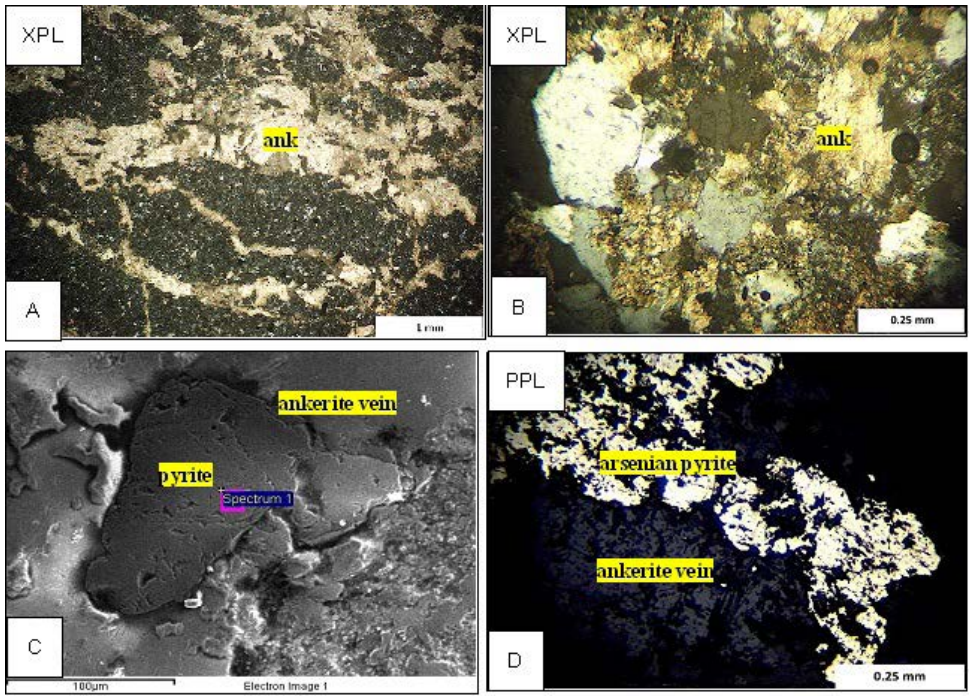

Figure 8: Carbonate alteration and sulfide mineralization present in JGD. Photo A is ankerite (ank) vein intersecting the mudrock unit. Photo B displays patches of ankerite (ank) replacing the clay matrix of siltstone. Photo C is a BSE image of Au-bearing pyrite in an ankerite vein. Photo D is a photomicrograph of arsenian pyrite in an ankerite vein.

minerals were formed syngenetic with carbonate minerals (Villareal-Tirona, 2022). The isocon diagram also suggests the enrichment of these elements (Au, Ca, Mg and Mn) during an alteration-mineralization event. Hence, it could be inferred that carbonate minerals and Au were introduced into the system during the main alteration-mineralization event. This differs from CTD, CLD, and even with known SHGD, where decalcification, followed by silicification, is crucial in Au deposition. Decalcification in JGD is challenging to identify using geochemistry because analysis lacks CaO and LOI (Loss of ignition). The decrease in CaO and LOI indicates decalcification in the system (Yigit & Hofstra, 2003). However, petrographic studies strongly suggest the absence of decalcification as well as the emplacement of silica through diagenesis and not hydrothermal in JGD (Villareal-Tirona, 2022). Furthermore, carbonate alteration is observed in most CTD distal from the central ore zone and barren of Au-bearing sulfide minerals (Hofstra, 1994 in Hofstra & Cline, 2000). Also, the source of H_2S responsible for the precipitation of sulfide minerals in these deposits suggests a strong influence from a magmatic source. In JGD, sulfur isotope reflects magmatic-hydrothermal origin (Goh, 2012; Kirwin & Royle, 2018). Also, earlier sulfur studies of the Pedawan Formation by Schuh (1993) suggest that another source of sulfur may have been from sedimentary sulfides. Statistical analysis indicates two possible origins of sulfur, i.e., (1) diagenetic and (2) alteration-mineralization process inferred to be due to hydrothermal-magmatic fluids, where the latter is strongly linked with Au mineralization. Likewise, similar to CTD, the Au-bearing pyrite in JGD results from the sulfidation process. Table 4 shows the comparison between major geologic features of CTD and JDG. Delineated limits of carbonate alteration and the portion of the mineralization zone with Au values of >1g/t in JGD are presented in Figure 9. Furthermore, the magmatic-arc setting and association with distal porphyry copper intrusive centers of JGD (Kirwin & Royle, 2018) differ from CTD.

CONCLUSION

Although the JGD displays similarities with CTD and CLD, there are several differences in (1) geologic setting and (2) association with porphyry copper intrusive. Also, geochemical and statistical studies show differences in (1) the association of Au mineralization assemblage (Au, As, Sb, S, and Bi) with carbonate alteration assemblage (Ca, Mg, and Mn), (2) the association of Bi with Au that is not common in CTD, and (3) elevated base metals. Given all the physical and chemical characteristics of JGD, it can be stated that the deposit is not coherent with the criteria of CTD or CLD and is most likely a SHGD, which agrees with the study conducted by Percival *et al*. (2018) in the BMD.

ACKNOWLEDGEMENTS

We extend our gratitude for the unwavering support of Besra Gold Inc. for providing the necessary data and information utilized in this study. Also, we would like to thank the reviewers for their valuable input in this paper.

AUTHORS CONTRIBUTION

AMVT and MIRBT conducted a field investigation and chose drill holes to be utilized for the statistical analysis. AVT and MIRBT performed statistical analysis on the geochemical data. AMVT wrote the manuscript. MIRBT and RS provided valuable input in the final form of the manuscript.

CONFLICT OF INTEREST

The authors have no conflicts of interest to declare that are relevant to the content of this article.

Table 4: Comparison of major features of Carlin-type deposits and Jugan gold deposit.

Features	Carlin-type deposits	Jugan gold deposit
Geologic setting	Passive margins	Magmatic arc overlain by thick sedimentary sequence
Geochemical signature	Au-Tl-As-Hg-Sb-(Te)	Au-As-Sb-S-Bi
Nature of Au	Solid solution in pyrite rims +/- native Au, rare arsenopyrite	Solid solution in pyrite
Intrusive association	Lack relationship with proximal upper crustal intrusion	Associated with porphyry copper intrusive
Alteration-mineralization	Decalcification, silicification, argillization	Silicification (diagenetic), carbonate alteration, argillization (intrusive)
Precipitation mechanism of Au	Sulfidation	Sulfidation
Fluid source	Probable magmatic	Magmatic-hydrothermal
References	Hofstra & Cline, 2000 Cline, 2018	Schuh (1993), Goh (2012) Kirwin & Royle (2018) This study

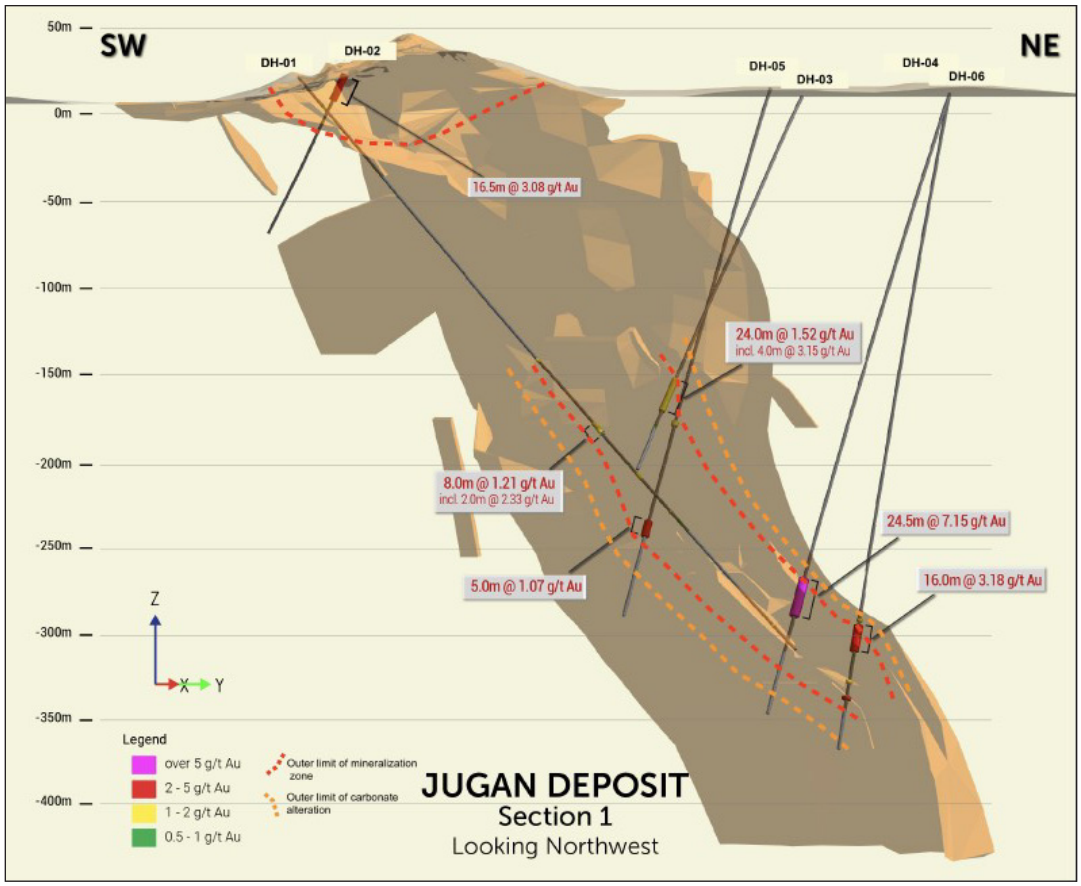

Figure 9: Cross section of the Jugan mineralization. The brown outline represents the mineralization envelope of the deposit. Modified from Besra Gold Inc., 2022.

REFERENCES

Baker, E.M., 1991. The timing and structural controls on the Carlin-Type mineralisation at Jugan (Bau, Sarawak) and implications for regional exploration. RGC Exploration Pty. Ltd. (Unpublished Report No. AWP 2/1991).

Banks, M.J., 2006. Prospectivity evaluation of the Bau Goldfield: Bukit Young Group properties, Sarawak, Malaysia. (Unpublished company report).

Besra Gold Inc., 2022. Geologic map of Jugan Gold Deposit and cross-section of Jugan mineralization [map]. https://www.besra.com/.

Breit, G.N., & Wanty, R.B., 1991. Vanadium accumulation in carbonaceous rocks: A review of geochemical controls during deposition and diagenesis. Chemical Geology, 91(2), 83-97.

Cline, J.S., 2018. Nevada's Carlin-type gold deposits: What we've learned during the past 10 to 15 years. In: J.L. Muntean (Ed.), Diversity of Carlin-style gold deposits. Society of Economic Geologists, Incorporated, Colorado. https://doi.org/10.5382/rev.20.

Garwin, S.L., 1996. The settings and styles of gold mineralisation in Southeast Asia. Bulletin of the Geological Society of Malaysia, 40, 77-111.

Garwin, S.L., 1996. The settings and styles of gold mineralisation in Southeast Asia. Geological Society of Malaysia Annual Geological Conference. Keynote Papers, 1-27.

Goh, K., 2012. Geological setting and mineralisation characteristics of the sedimentary rock hosted disseminated Jugan Au deposit, Bau Mining District, Sarawak, Malaysia. University of Tasmania BSc Thesis, unpublished.

Hall, R., van Hattum, M.W., & Spakman, W., 2008. Impact of India–Asia collision on SE Asia: The record in Borneo. Tectonophysics, 451(1-4), 366-389.

Hall, R., & Nichols, G., 2002. Cenozoic sedimentation and tectonics in Borneo: Climatic influences on orogenesis. Geological Society London, Special Publication, 191(1), 5-22.

Hamilton, W.B., 1979. Tectonics of the Indonesian region. USGS Professional Paper 1078, 356 p.

Hofstra, A.H., 1994. Geology and genesis of the Carlin-type gold deposits in the Jerritt Canyon district, Nevada. Ph.D. dissertation, University of Colorado, Boulder. 719 p.

Hofstra, A.H., & Cline, J.S., 2000. Characteristics and models for Carlin-type gold deposits. Reviews in Economic Geology, 13, 163-220.

Hutchison, C.S., 1996. The 'Rajang accretionary prism' and 'Lupar Line' problem of Borneo. Geological Society London Special Publication, 106(1), 247-261.

Hutchison, C.S., 2005. Geology of North-West Borneo: Sarawak, Brunei and Sabah. Elsevier. 444 p.

Japan International Cooperative Agency (JICA) Metal Mining Agency of Japan, 1985. Report on the collaborative mineral exploration of the Bau area, West Sarawak. 23-24p. https://openjicareport.jica.go.jp/pdf/10313211_01.pdf.

Kirwin, D.J., & Ingram, P.A., 1993. Technical notes concerning a visit to the Bau Goldfield, Sarawak, East Malaysia. Menzies Gold N.L. (Unpublished Company Report).

Kirwin, D.J., & Royle, D.Z., 2018. Sediment-hosted gold deposits in Southeast Asia. Resource Geology, 69(2), 125-147.

Li, Z., & Peters, S.G., 1998. Comparative geology and geochemistry of sedimentary rock-hosted (Carlin-type) gold deposits in the People's Republic of China and in Nevada. USGS Open-File Report 98-466, 1-91.

Li, S., Xia, Y., Liu, J., Xie, Z., Tan, Q., Zhao, Y., & Guo, H., 2019. Geological and geochemical characteristics of the Baogudi Carlin-type gold district (Southwest Guizhou, China) and their geological implications. Acta Geochimica, 38(4), 587-609.

Marjoribanks, R.W., 1986. Assessment of the gold potential of the Bau district, Sarawak, Malaysia. GFAL Report, 14 p. (unpublished).

Mustard, H., 1997. The Bau Gold district, AusIMM. World Gold Conference '97, Singapore. 21 p.

Patterson, L.M., Muntean, J.L., Steininger, R.C., & Pennell, W.M., 2011. Multi-element geochemistry across a Carlin-type gold district: Jerritt Canyon, Nevada. In: Great Basin Evolution and Metallogeny. Geological Society of Nevada 2010 Symposium Proceedings, Reno, 1119, 1152.

Percival, T.J., Radtke, A.S., & Bagby, W.C., 1990. Relationships among carbonate replacement gold deposits, gold skarns, and intrusive rocks, Bau Mining District, Sarawak, Malaysia. Mining Geology, 40(1), 1-16.

Percival, T.J., Hofstra, A.H., Gibson, P.C., Noble, D.C., Radtke, A.S., Bagby, W.C., & McKee, E.H., 2018. Sedimentary rock-hosted gold deposits related to epizonal intrusions, Bau district, Island of Borneo, Sarawak, East Malaysia. Reviews in Economic Geology, 20, 259-297.

Pour, A.B., Hashim, M., & van Genderen, J., 2013. Detection of hydrothermal alteration zones in a tropical region using satellite remote sensing data: Bau goldfield, Sarawak, Malaysia. Ore Geology Reviews, 54, 181-196.

Schuh, W.D., 1993. Geology, geochemistry, and ore deposits of the Bau gold mining district, Sarawak, Malaysia. Ph.D. thesis, University of Arizona. 445 p.

Sethi, P.S., & Schieber, J., 1998. Economic aspects of shales and clays: An overview. In: Jürgen Schieber, Winfried Zimmerle, & Parvinder S. Sethi (Eds.), Shales and mudstones, II. Schweizerbart Science Publisher, Stuttgart, Germany. 237-253.

Sillitoe, R.H., 1986. Mineralisation styles and exploration potential of the Bau Gold District, Sarawak, Malaysia. Unpublished report for GFAL. 13 p.

Simon, G., Kesler, S.E., & Chryssoulis, S., 1999. Geochemistry and textures of gold-bearing arsenian pyrite, Twin Creeks, Nevada; Implications for deposition of gold in Carlin-type deposits. Economic Geology, 94(3), 405-421.

Stenger, D.P., Kesler, S.E., Peltonen, D.R., & Tapper, C.J., 1998. Deposition of gold in Carlin-type deposits; The role of sulfidation and decarbonation at Twin Creeks, Nevada. Economic Geology, 93(2), 201-215.

Van Hattum, M. W.A., 2005. Provenance of Cenozoic sedimentary rocks of northern Borneo. Ph.D Thesis. The University of London. 457 p.

Venendaal, J.F., 2007. Trace element geochemistry and carbonate alteration as indicators for gold mineralization at the Cortez Hills deposit, Lander County, Nevada. MSc Thesis, Colorado School of Mines. 128 p.

Villareal-Tirona, A.M., 2022. Geochemical and petrographic characteristics of the Jugan gold deposit, Sarawak, Malaysia. MSc Thesis, The University of the Philippines-Diliman, unpublished.

Wolfenden, E.B., 1965. Bau mining district, West Sarawak, Malaysia, Part 1. Bulletin, Malaysia Geol. Survey Borneo Region, 7, 147p.

Yigit, O. & Hofstra, A.H., 2003. Lithogeochemistry of Carlin-type gold mineralization in the Gold Bar district, Battle Mountain-Eureka trend, Nevada. Ore Geology Reviews, 22(3-4), 201-224.

Manuscript received 29 April 2022;
Received in revised form 12 September 2022;
Accepted 23 September 2022
Available online 30 November 2022